Tellus (1978), *30*, 1–14

Linear and nonlinear contributions to the growth and decay of the large-scale atmospheric waves and jet stream

By CHING-YEN TSAY[1] and S.-K. KAO, *Department of Meteorology, University of Utah, Salt Lake City, Utah 84112, U.S.A.*

(Manuscript received March 8, 1977)

ABSTRACT

To study the growth and decay of the atmospheric wave motions in middle latitudes, we have analyzed the mechanism for the kinetic energy change in wavenumber domain, and computed the composite average of each term in the kinetic energy equation at various stages in the life cycle of the atmospheric waves. It is found that for the first 1 to 2 days the extra-long waves of wavenumbers 1 and 3 grow by receiving kinetic energy from other finite amplitude waves through nonlinear interactions; in the next 1 to 2 days, they grow by gaining energy through nonlinear interactions and converting available potential to kinetic energy. These waves then maintained their peak energy for 3 to 4 days through the balance between the energy supply from conversion of available potential energy to kinetic energy and nonlinear interactions, and the energy lost by dissipation. The contribution of nonlinear interactions then changes to negative; and in the next 3 to 4 days, the waves decay by losing energy through nonlinear interactions and dissipation. The average life cycle of these extra-long waves is about 10 to 11 days. Similar results have been found with regard to the synoptic-scale waves of wavenumbers 4 to 8. They also intensify by receiving energy and decay by losing energy through nonlinear interactions among finite amplitude waves. Nevertheless, the conversion of the available potential energy to kinetic energy plays a more important role in the growing stage of the synoptic-scale waves than for the extra-long waves. The average life cycle for the synoptic-scale waves is about 6 to 8 days. It is interesting to note that the characteristics of waves of wavenumber 2 are quite different from those of the other waves. In all stages of its life cycle, the contribution of nonlinear interactions is negative and the conversion term always has large positive values.

We have also analyzed the intensification and decay of the subtropical jet stream, and found that it is greatly affected by the convergence and divergence of eddy momentum flux. The fluctuations of the net momentum flux are mainly contributed by the synoptic-scale waves of wavenumbers 4 to 8.

1. Introduction

Analyses of the mechanism of the growth and decay of waves and zonal mean motion are essential to the understanding of weather changes in the atmosphere. The growth and decay of atmospheric motions may be contributed by linear and nonlinear mechanisms. For unstable waves of small amplitude in a barotropic fluid, it is known that their growth is generally at the expense of the kinetic energy of the zonal mean flow. In a baroclinic atmosphere, however, an amplify wave of small amplitude receives available potential energy from the zonal mean motion and at the same time, converts it to kinetic energy. The linear theory is able to describe time changes of a system very well while disturbances remain small, but not after they become finite in amplitudes. For waves of finite amplitude, the nonlinear transfers of energies become complex. In a barotropic fluid, interactions of two-dimensional waves of finite amplitude transfer a large portion of the kinetic energy to waves of larger scale and a small fraction of the energy to those of smaller scale (Fjørtoft, 1953), and the exchanges of kinetic energy between a zonal flow and two waves lead to a process similar

[1] On leave from the Department of Atmospheric Sciences, National Taiwan University, Taipei, Taiwan, Republic of China.

to that of the index cycle in the atmosphere (Lorenz, 1960). Indeed, nonlinear interactions play an important role in the transfer of kinetic energy in wave motion.

Because of the effects of baroclinicity and topography of the earth's surface, the linear and nonlinear interactions of waves in the atmosphere are much more complex. In addition, the mathematical complexity also adds difficulty to the understanding of the characteristics of atmospheric waves. It is felt that in order to understand properly the mechanism for the large-scale wave motion in the atmosphere, it is necessary to analyze the processes of energy transfers in the real atmosphere. One of the fruitful approaches to such an analysis is to examine the atmospheric processes with the use of Fourier transformed governing equations. Spectral energy equations in wavenumber domain were first formulated by Saltzman (1957). His study was followed by a number of observational studies (e.g. Saltzman & Fleisher, 1960, 1961; Yang, 1967; Steinberg et al. 1971; Tenenbaum, 1976; Burrows, 1976). Spectral energetics have also been examined in the frequency domain (Tsay & Kao, 1973, 1974) and in the wavenumber-frequency domain (e.g. Kao, 1968; Wendell, 1969; Kao & Wendell, 1970; Kao & Lee, 1977).

Analyses of the meteorological observations in wavenumber domain indicate that the zonal mean flow generally transfers its available potential energy gained from the zonal mean radiative heating to waves of various wavenumber. Part of the eddy available potential energy is converted to eddy kinetic energy, and part of the latter is transferred to the zonal mean flow. The nonlinear interactions transfer kinetics energy from the synoptic-scale waves to longer except wavenumber 2 and shorter waves (Saltzman, 1970). Analyses of the data in wavenumber-frequency domain indicate that the nonlinear interactions generally supply kinetic energy to waves moving in the direction of the mean zonal flow, but extract kinetic energy from waves moving in the opposite direction of the mean flow (Kao & Lee, 1977).

These studies have provided valuable information regarding the seasonal averages of the atmospheric processes for the large-scale wave motion in the atmosphere. However, to understand the mechanism for the growth and decay of the wave motion, it is necessary to analyze the conversion, transfer, and dissipation of the available potential and kinetic energies at various stages of the life cycle of the atmospheric waves. The main objective of this paper is to make such a study.

2. Notations and equations

In this study, $q(\lambda, \phi, p, t)$ is considered as an arbitrary atmospheric quantity, where λ, ϕ, p and t stand for longitude, latitude, pressure, and time. For brevity, $q(\lambda, \phi, p, t)$ is denoted by $q(\lambda)$. Its Fourier transform pair in wavenumber space is as follows

$$Q(n) = Q_c(n) + iQ_s(n) = \frac{1}{2\pi}\int_0^{2\pi} q(\lambda)\, e^{-in\lambda}\, d\lambda$$

$$q(\lambda) = \sum_{n=-\infty}^{\infty} Q(n)\, e^{in\lambda}$$

where λ is normalized to 2π, n represents nondimensional integer wavenumber, and $Q(n)$ has the same unit as $q(\lambda)$. The following notations for the transforms will be used

$q(\lambda)$	u	v	ω	z	T
$Q(n)$	U	V	Ω	Z	Θ

where, u and v are eastward and northward wind speed, $\omega = dp/dt$ is vertical pressure velocity, z is height of an isobaric surface, and T is temperature. We would also like to mention here that notations of R, a, and g respectively represent gas constant, radius of the earth, and acceleration of gravity.

Equations for the rate of change of the globally integrated kinetic energy in wavenumber space were first derived by Saltzman (1957) and could also be found in his review paper (Saltzman, 1970). In the present study, we apply the same equations, except we only integrate them over a latitude belt at a pressure surface. Consequently, additional boundary flux terms would appear in the present forms of equations. In addition, the unit of $(m/s)^2$ will be adopted for the kinetic energy per unit mass in wavenumber space. The equation of zonal kinetic energy per unit mass in a computational form is as follows

$$\frac{\partial}{\partial t}K(0) = \sum_{n=1}^{\infty} M_1(n) + \sum_{n=1}^{\infty} M_2(n) + \sum_{n=1}^{\infty} M_3(n) + C(0) - D(0) + BVZ(0) + BWZ(0) + BVK(0) + BWK(0) + \sum_{n=1}^{\infty} F_1(n) + \sum_{n=1}^{\infty} F_2(n) \quad (1)$$

where

$$K(0) = \frac{1}{b}\int_{\phi_S}^{\phi_N} K(0, \phi)\cos\phi\, d\phi,$$

$$K(0, \phi) = \frac{1}{2}(\bar{u}^2 + \bar{v}^2),$$

the kinetic energy of the zonal mean motion;

$$M_1(n) = \frac{1}{b}\int_{\phi_S}^{\phi_N}\left\{\left[\frac{\cos\phi}{a}\frac{\partial}{\partial\phi}\left(\frac{\bar{u}}{\cos\phi}\right)\right]\Phi_{UV}(n)\right\}\cos\phi\, d\phi,$$

$$M_2(n) = \frac{1}{b}\int_{\phi_S}^{\phi_N}\{\bar{u}_p\Phi_{U\Omega}(n)\}\cos\phi\, d\phi,$$

$$M_3(n) = \frac{1}{b}\int_{\phi_S}^{\phi_N}\left\{\frac{1}{a}\bar{v}_\phi\,\Phi_{VV}(n) + \bar{v}_p\Phi_{V\Omega}(n) - \frac{\tan\phi}{a}\bar{v}\Phi_{UU}(n)\right\}\cos\phi\, d\phi,$$

contributions of interaction between waves of wavenumber n and the mean meridional motion;

$$C(0) = -\frac{R}{bp}\int_{\phi_S}^{\phi_N}\bar{\omega}\bar{T}''\cos\phi\, d\phi,$$

the rate of conversion between the available potential and kinetic energies of the zonal mean motion;

$$BVZ(0) = -\frac{g}{ba}[\bar{v}\bar{z}''\cos\phi]_{\phi_S}^{\phi_N},$$

$$BWZ(0) = -\frac{g}{b}\int_{\phi_S}^{\phi_N}\left[\frac{\partial}{\partial p}(\bar{\omega}\bar{z}'')\right]\cos\phi\, d\phi,$$

the net boundary fluxes of mean potential energy;

$$BVK(0) = -\frac{1}{ba}[\bar{v}K(0, \phi)\cos\phi]_{\phi_S}^{\phi_N},$$

$$BWK(0) = -\frac{1}{b}\int_{\phi_S}^{\phi_N}\left\{\frac{\partial}{\partial p}[\bar{\omega}K(0, \phi)]\right\}\cos\phi\, d\phi,$$

the net boundary fluxes of mean kinetic energy;

$$F_1(n) = -\frac{1}{ba}\{[\bar{u}\Phi_{UV}(n) + \bar{v}\Phi_{VV}(n)]\cos\phi\}_{\phi_S}^{\phi_N},$$

$$F_2(n) = -\frac{1}{b}\int_{\phi_S}^{\phi_N}\left\{\frac{\partial}{\partial p}[\bar{u}\Phi_{U\Omega}(n) + \bar{v}\Phi_{V\Omega}(n)]\right\}\cos\phi\, d\phi,$$

the net boundary fluxes arising from interaction between waves of wavenumber n and the zonal mean motion;

and

$b = (\sin\phi_N - \sin\phi_S)$;

$\Phi_{RQ}(n) = 2[R_c(n)Q_c(n) + R_s(n)Q_s(n)]$.

For an arbitrary atmospheric quantity q:

$\bar{q} = \frac{1}{2\pi}\int_0^{2\pi} q\, d\lambda$, zonal average of q;

$\tilde{q} = \frac{1}{b}\int_{\phi_S}^{\phi_N} q\cos\phi\, d\phi$, meridional average of q;

$q'' = q - \tilde{q}$, deviation from the meridional average;

$q_\phi = \partial q/\partial\phi$, derivative with respect to ϕ;

$q_p = \partial q/\partial p$, derivative with respect to p.

The equation of eddy kinetic energy per unit mass in wavenumber domain in a computational form is as follows:

$$\frac{\partial}{\partial t}K(n) = L_1(n) + L_2(n) - M_1(n) - M_2(n) - M_3(n) + C(n) - D(n) + BVZ(n) + BWZ(n) + BVK(n) + BWK(n) + BL1(n) + BL2(n) \qquad (2)$$

where

$$K(n) = \frac{1}{b}\int_{\phi_S}^{\phi_N} K(n, \phi)\cos\phi\, d\phi,$$

$$K(n, \phi) = \tfrac{1}{2}[\Phi_{UU}(n) + \Phi_{VV}(n)],$$

the kinetic energy of waves of wavenumber n;

$$L_1(n) = \frac{1}{b}\int_{\phi_S}^{\phi_N}\left\{\frac{n}{a\cos\phi}[\psi^{(2)}_{UUV}(n) + \psi^{(2)}_{VVU}(n)] + \frac{1}{a}\left[\Psi^{(1)}_{UU_\phi V}(n) + \psi^{(1)}_{VV_\phi V}(n)\right] + \frac{\tan\phi}{a}\left[\psi^{(1)}_{VUU}(n) - \psi^{(1)}_{UVU}(n)\right]\right\}\cos\phi\, d\phi,$$

$$L_2(n) = \frac{1}{b}\int_{\phi_S}^{\phi_N}\left[\psi^{(1)}_{UU_p\Omega}(n) + \psi^{(1)}_{VV_p\Omega}(n)\right]\cos\phi\, d\phi,$$

nonlinear interaction contributions to waves of wavenumber n;

$$C(n) = -\frac{R}{bp}\int_{\phi_S}^{\phi_N}\left[\Phi_{\Omega\Theta}(n)\cos\phi\right]d\phi,$$

the rate of conversion between the available potential and kinetic energies of waves of wavenumber n

$$BVZ(n) = -\frac{g}{ba}\left[\Phi_{VZ}(n)\cos\phi\right]_{\phi_S}^{\phi_N},$$

$$BWZ(n) = -\frac{g}{b}\int_{\phi_S}^{\phi_N}\left[\frac{\partial}{\partial p}\Phi_{\Omega Z}(n)\right]\cos\phi\, d\phi,$$

the net boundary fluxes of potential energy of waves of wavenumber n;

$$BVK(n) = -\frac{1}{ba}\left[\bar{v}K(n,\phi)\cos\phi\right]_{\phi_S}^{\phi_N},$$

$$BWK(n) = -\frac{1}{b}\int_{\phi_S}^{\phi_N}\left[\frac{\partial}{\partial p}\bar{\omega}K(n,\phi)\right]\cos\phi\, d\phi,$$

the net boundary fluxes of kinetic energy of waves of wavenumber n;

$$BL1(n) = -\frac{1}{ba}\left\{[\psi^{(1)}_{UUV}(n) + \psi^{(1)}_{VVV}(n)]\cos\phi\right\}_{\phi_S}^{\phi_N}$$

$$BL2(n) = -\frac{1}{b}\int_{\phi_S}^{\phi_N}\frac{\partial}{\partial p}\left[\psi^{(1)}_{UU\Omega}(n) + \psi^{(1)}_{VV\Omega}(n)\right]\cos\phi\, d\phi$$

the net boundary fluxes arising from nonlinear interactions among waves;
and

$$\psi^{(1)}_{RQP}(n) = 2Q_c(n)[H^{(1)}_{RP}(n) + H^{(2)}_{RP}(n)] + 2Q_S(n)[H^{(3)}_{RP}(n) + H^{(4)}_{RP}(n)];$$

$$\psi^{(2)}_{RQP}(n) = -2Q_c(n)[H^{(3)}_{RP}(n) + H^{(4)}_{RP}(n)] + 2Q_S(n)[H^{(1)}_{RP}(n) + H^{(2)}_{RP}(n)];$$

$$H^{(1)}_{RP}(n) = \sum_{m=1}^{\infty}[R_c(m)P_c(n+m) + R_S(m)P_S(n+m) + R_c(n+m)P_c(m) + R_S(n+m)P_S(m)];$$

$$H^{(2)}_{RP}(n) = \sum_{m=1}^{N} w[R_c(m)P_c(n-m) - R_s(m)P_s(n-m) + R_c(n-m)P_c(m) - R_s(n-m)P_s(m)];$$

$$H^{(3)}_{RP}(n) = \sum_{m=1}^{\infty}[R_c(m)P_S(n+m) - R_S(m)P_c(n+m) + R_S(n+m)P_c(m) - R_c(n+m)P_S(m)];$$

$$H^{(4)}_{RP}(n) = \sum_{m=1}^{N} w[R_c(m)P_S(n-m) + R_S(m)P_c(n-m) + R_c(n-m)P_S(m) + R_S(n-m)P_c(m)];$$

$$\begin{cases} 0.5 & \text{if } n \text{ is even and } m = n/2 \\ 1 & \text{otherwise;} \end{cases}$$

$$\begin{cases} n/2 & \text{if } n \text{ is even} \\ (n-1)/2 & \text{if } n \text{ is odd.} \end{cases}$$

3. Data and computations

Northern hemisphere octagonal grid data on 500 and 200 mb from National Meteorological Center (NMC) are used in this study. The period from 00GMT 1 December 1975 through 12 GMT 29 February 1976 is selected. Wind, height and temperature data are 12 hourly analysis values. The analyzed wind fields are essentially nondivergent and the mean meridional circulation is zero. The data of ω field at 00 and 12 GMT are linearly interpolated values from the available 4th to 6th hour averaged forecasting ω values. The ω field is used only for the computation of the rate of conversion between available potential and kinetic energies. As will be seen later, the seasonal and composite average values of the conversion term seem reasonable. All the octagonal grid data are interpolated by a 4-point double linear scheme to a 2.5° resolution grid. In addition to the northern hemisphere data, NMC tropical grid temperature data in the same period are also used for the computation of northern hemisphere mean temperature.

Eq. (2) is used for the computation of wave energetics on 500 mb. The domain of integration is 30° to 60° N, which represents middle latitudes. The term of the rate of change of kinetic energy is computed by a centered finite differencing scheme from the 12 hourly analyzed wave kinetic energy, whereas, the derivatives with respect to latitudes are computed from a 2.5° latitude resolution grid. The terms involving vertical advection and the mean meridional circulation, i.e. $L_2(n)$, $M_2(n)$, $M_3(n)$, $BWZ(n)$, $BWK(n)$ and $BL2(n)$ are not computed. Therefore, the residue term will include dissipation, data and computational errors, and all those uncomputed terms. Those uncomputed terms and the errors should be small because the residue term behaves similarly to the dissipation.

Eq. (1) is computed similarly for the study of the energetics of zonal mean motion on 200 mb. The domain of integration is 20° to 45° N, which covers latitudes of maximum mean zonal motion (see Fig. 4). The terms involving vertical advection and the mean meridional circulation, i.e. $M_2(n)$, $M_3(n)$, $BVZ(0)$, $BWZ(0)$, $BVK(0)$, $BWK(0)$, $F_2(n)$ and second part of $F_1(n)$ are not computed. However, seasonal average of $BVK(0)$ and $BWK(0)$ could be estimated. The other uncomputed terms should be small.

Time oscillations of kinetic energy of waves and

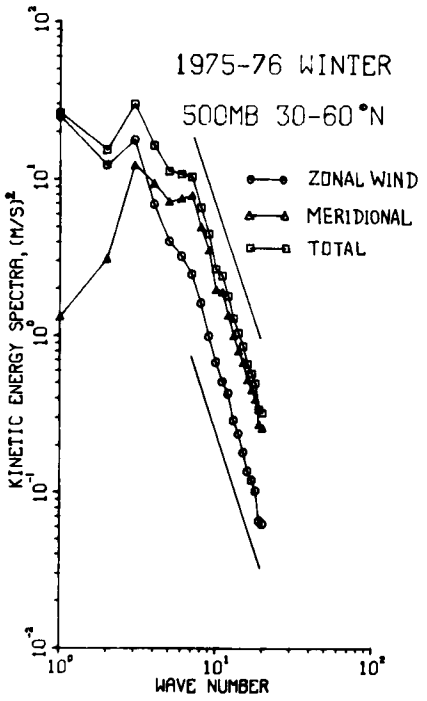

Fig. 1. Seasonal average kinetic energy spectra in wavenumber domain. The two straight lines have n^{-3} dependence.

zonal mean motion could be easily seen in Figs. 2 and 5, respectively. Composite studies are conducted to investigate the amplitude increasing and decreasing mechanisms of waves and zonal mean motion. Each cycle of time oscillations is divided into five stages. Stages I and II are energy increasing stages with their kinetic energies respectively smaller than 0.5, and within 0.5 to 0.85 times of the peak energy in the cycle. Stage III is a stage with its kinetic energy larger than 0.85 times of the peak energy; whereas, stages IV and V are energy decreasing stages with their kinetic energies respectively within 0.5 to 0.85, and smaller than 0.5 times of the peak energy. Time average in each stage is computed for each term of the kinetic energy equations. Composite averages of several cases are then calculated for the five stages.

4. Energetics of wave motions

To provide a background for the analysis of the mechanism for the growth and decay of wave amplitudes at 500 mb, a brief discussion of the seasonal average statistics is in order. We shall first examine the seasonal averaged kinetic energy spectra in wavenumber domain. Fig. 1 shows that in the wavenumber range between 7 and 20 the energy spectra of both the zonal and meridional components of the velocity are approximately proportional to the minus three power of the wave number. In the low wavenumber end, the energy spectrum of the zone velocity generally decreases with increasing wavenumber, whereas that of the meridional velocity shows an energy peak between wavenumbers 3 and 7. These spectral characteristics are similar to those observed in earlier studies (e.g. Wiin-Nielsen, 1967; Kao & Wendell, 1970).

Table 1. *Seasonal average contributions to the rate of change of wave kinetic energy for 30°–60° N, 500 mb, winter 1975–76. Unit in* $(m/s)^2\ day^{-1}$

Wave number \ Terms dK/dt	L_1-M_1		C	BVZ	$BL1$	RES
1	.1	5.7	−.3	4.1	−.3	−2.9	−6.3
2	−.1	−2.9	−.5	13.8	−.1	1.3	−11.7
3	.1	3.5	−.5	8.3	−1.0	.0	−10.5
4	.1	−.3	.3	5.3	−1.1	.2	−4.3
5	.0	−2.2	.0	5.9	−.7	.7	−3.6
6	−.1	−2.0	−.3	6.3	−.8	.5	−3.8
7	−.2	−.6	−.2	8.1	−1.4	−.1	−5.9
8	.0	−.6	−.1	7.7	−.4	−.7	−6.0
9	.0	.0	−.1	4.1	−.5	−.4	−3.4
10	.0	−.4	.0	2.2	.1	.1	−2.0
11	.0	−.2	−.0	1.6	−.1	.1	−1.4
12	.0	.0	−.0	1.5	.0	.0	−1.5
13	.0	−.1	−.0	.9	−.2	−.1	−.5
14	.0	.1	−.0	.4	.0	.1	−.6
15	.0	.0	−.0	.5	.0	−.1	−.4
16	.0	.2	−.0	.4	.0	.0	−.5
17	.0	.1	−.0	.2	−.1	.0	−.3
18	.0	.2	−.0	.2	.0	.0	−.4
19	.0	.1	−.0	.2	.0	.0	−.3
20	.0	.2	−.0	.1	.0	.0	−.3

As an aid to the analysis of the seasonal mean linear and nonlinear contributions to the rate of change of spectral kinetic energy, listed in Table 1 are values of contributions to the rate of change of spectral energy due to the nonlinear interactions among waves (L_1), interaction between waves and zonal mean motion ($-M_1$), conversion from the available potential energy to the kinetic energy (C), fluxes of potential energy (BVZ) and of those arising from the nonlinear interactions among waves through boundaries ($BL1$), and due to the

effects of dissipation including the Reynolds stress force, data and computational errors and the uncomputed terms (RES). It is seen from this table that the characteristics of the seasonal averaged transfers of energies are in general agreement with those reported by Saltzman (1970). Both the extra-long waves of wavenumbers 1 and 3, and shorter waves of wavenumbers 14 to 20 gain energy from synoptic-scale waves of wavenumbers 4 to 13 and from the extra-long wave of wavenumber 2 (L_1 being positive for energy gaining waves and negative for energy losing waves). The magnitudes of our results could also be compared with Saltzman's (1970) vertically integrated results, if we assume values at 500 mb are approximately equal to that of vertical averages and if values in Table 1 are multiplied by p_0/g. For $p_0 = 1000$ mb, our values of L_1, C, and RES are respectively about 1.9, 2.7, and 2.2 times larger than those reported by Saltzman. The discrepancy in the magnitude is probably due to the fact that wave motions between 30° and 60° N at 500 mb are generally stronger than that of the global average, and could also be a result of the stronger wave activities in our observational period. Since the term L_1 could be computed accurately from the observed horizontal wind fields and our values of C and L_1 are both about double those of Saltzman, we believe that the NMC forecasted ω field is good enough for qualitative discussions of the conversion term C. It is also seen in Table 1 that the residue term is negative for all wavenumbers. If eddy kinetic energy decays exponentially with time by the rate of the residue term, then the e-folding decay time for the seasonal averaged total eddy kinetic energy is about 2.5 days, which is of the same order of magnitude as the spin-down time (4 days) estimated by Holton (1972). Since the residue term behaves like a dissipation term, we may infer that data and computational errors, and contributions from those uncomputed terms are rather small.

Although the seasonal averaged results can describe well the maintenance of the general circulation in the atmosphere, they cannot explain the time evolution of wave amplitudes. In the atmosphere, intensification and weakening of a weather system are commonly observed synoptic phenomena. For a better understanding of the life cycle of wave motion, the time evolutions of kinetic energies of large-scale waves are shown in Fig. 2. The time oscillations of wave amplitudes are clearly seen. It may be noted that the oscillation periods for extra-long waves ($n = 1$, 2, and 3) range from 5 to 17 days, while those for synoptic-scale waves ($n = 4 - 8$) from 4 to 11 days. Amplitude oscillations of waves at 200 mb (not shown) are similar and in phase with those at 500 mb. Several significant cycles for each wavenumber are selected for the study of the mechanism for the growth and decay of wave amplitude. It may be pointed out that terms in equation (2) are computed at every 12 h of observation time and that composite averages (as discussed in section 3) are calculated for five stages of the life cycle of waves of each wavenumber. The averaged contributions to the rate of change of wave kinetic energy at the five stages are shown in Table 2. The contributions of nonlinear interaction components at amplitude increasing (stage I + II) and decreasing (stage IV + V) stages are shown in Fig. 3. Discussions of these contributions to waves of various wavenumbers are made in the following subsection.

4.1 *Extra-long waves of wavenumber 1 and 3*

Composite averages for wavenumber 1 and 3 are shown in Tables 2a and 2c, respectively. As was described earlier, the rate of change of wave kinetic energy, dK/dt, is positive in stages I and II and negative in stages IV and V. Surprisingly, we found that the nonlinear term, L_1, is also positive in stages I and II, and negative in stages IV and V, indicating that the nonlinear interactions among waves (L_1) contribute greatly to the growth and decay of waves of wavenumbers 1 and 3. It is also interesting to find that the conversion term, C, is negligible in stage I and positive in other stages with a maximum value in stage III. The residue term, on the other hand, is negative in all stages and roughly cancels the contribution made by the conversion term. The transfer of kinetic energy from these extra-long waves to zonal mean motion, M_1, is generally small.

The amplitude oscillations of the extra-long waves may, therefore, be explained as follows. In the first 1 to 2 days (stage I) of the life cycle, the extra-long waves of wavenumbers 1 and 3 essentially grow by receiving kinetic energy from other waves through nonlinear interactions. They continue to grow for the next 1 to 2 days (stage II) by gaining energy through nonlinear interactions and through converting available potential energy to kinetic energy. These waves then maintained their peak energy for 3 to 4 days (stage III), as a consequence of the balance between the energy

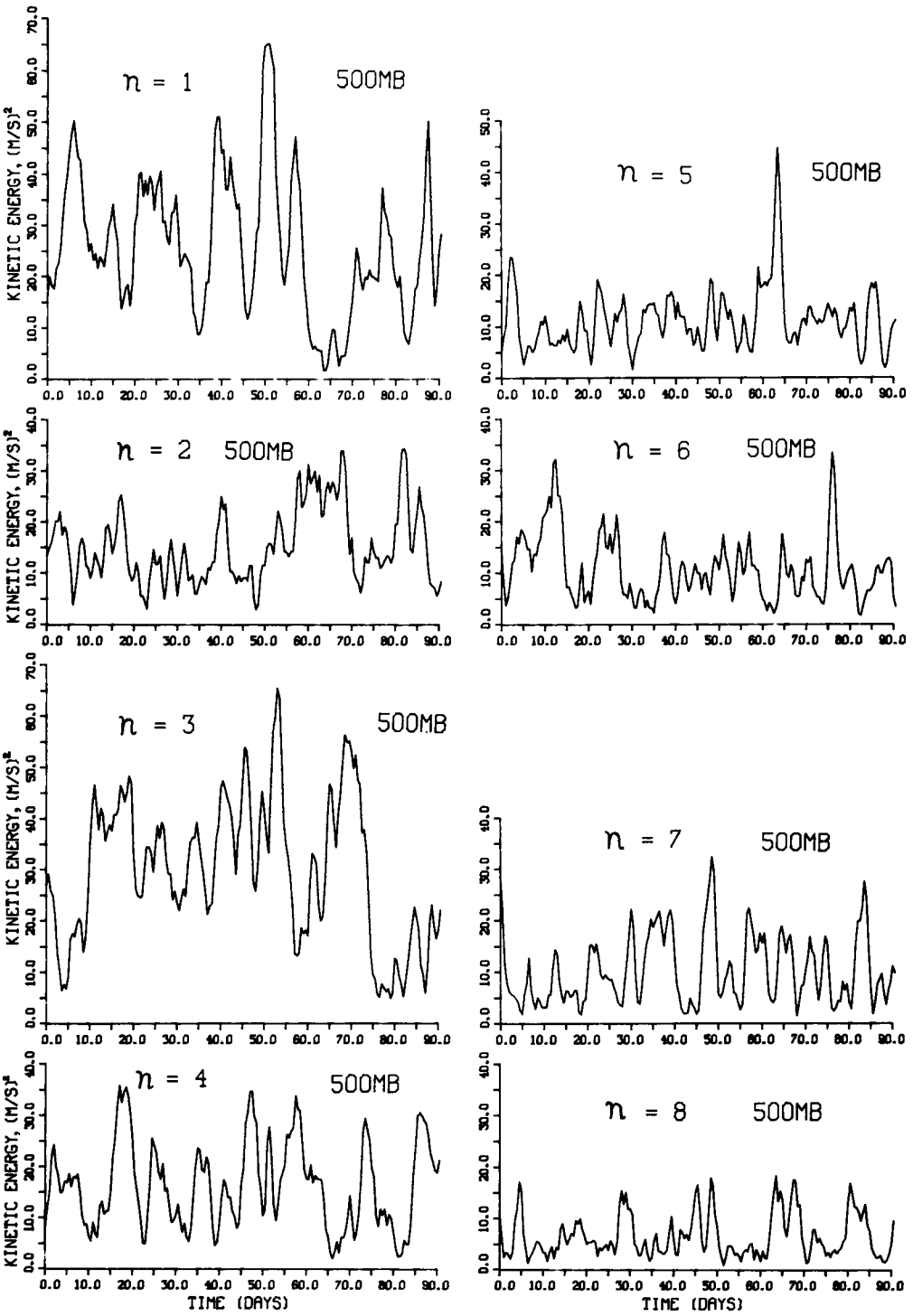

Fig. 2. Time evolutions of kinetic energies of large-scale waves in the period of 1 December 1975 00Z to 29 February 1976 12Z.

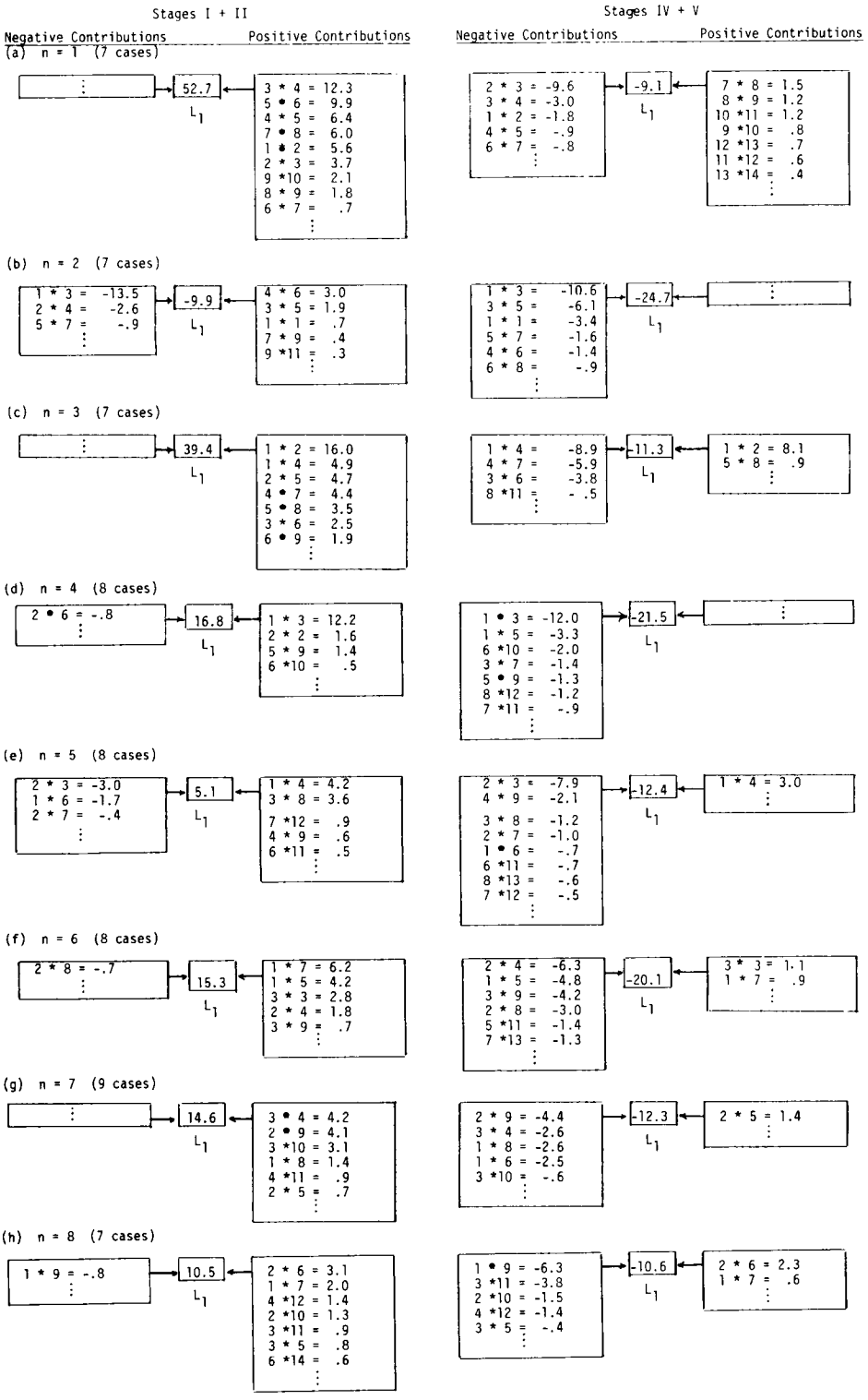
Stages I + II
Negative Contributions
Positive Contributions
Stages IV + V
Negative Contributions
Positive Contributions
(a) n = 1 (7 cases)
52.7
L1
3 * 4 = 12.3
5 • 6 = 9.9
4 * 5 = 6.4
7 • 8 = 6.0
1 • 2 = 5.6
2 * 3 = 3.7
9 *10 = 2.1
8 * 9 = 1.8
6 * 7 = .7
2 * 3 = -9.6
3 * 4 = -3.0
1 * 2 = -1.8
4 * 5 = -.9
6 * 7 = -.8
-9.1
L1
7 * 8 = 1.5
8 * 9 = 1.2
10 *11 = 1.2
9 *10 = .8
12 *13 = .7
11 *12 = .6
13 *14 = .4
(b) n = 2 (7 cases)
1 * 3 = -13.5
2 * 4 = -2.6
5 * 7 = -.9
-9.9
L1
4 * 6 = 3.0
3 * 5 = 1.9
1 * 1 = .7
7 * 9 = .4
9 *11 = .3
1 * 3 = -10.6
3 * 5 = -6.1
1 * 1 = -3.4
5 * 7 = -1.6
4 * 6 = -1.4
6 * 8 = -.9
-24.7
L1
(c) n = 3 (7 cases)
39.4
L1
1 * 2 = 16.0
1 * 4 = 4.9
2 * 5 = 4.7
4 • 7 = 4.4
5 • 8 = 3.5
3 * 6 = 2.5
6 • 9 = 1.9
1 * 4 = -8.9
4 * 7 = -5.9
3 * 6 = -3.8
8 *11 = - .5
-11.3
L1
1 * 2 = 8.1
5 * 8 = .9
(d) n = 4 (8 cases)
2 • 6 = -.8
16.8
L1
1 * 3 = 12.2
2 * 2 = 1.6
5 * 9 = 1.4
6 *10 = .5
1 • 3 = -12.0
1 * 5 = -3.3
6 *10 = -2.0
3 * 7 = -1.4
5 • 9 = -1.3
8 *12 = -1.2
7 *11 = -.9
-21.5
L1
(e) n = 5 (8 cases)
2 * 3 = -3.0
1 * 6 = -1.7
2 * 7 = -.4
5.1
L1
1 * 4 = 4.2
3 * 8 = 3.6
7 *12 = .9
4 * 9 = .6
6 *11 = .5
2 * 3 = -7.9
4 * 9 = -2.1
3 * 8 = -1.2
2 * 7 = -1.0
1 • 6 = -.7
6 *11 = -.7
8 *13 = -.6
7 *12 = -.5
-12.4
L1
1 * 4 = 3.0
(f) n = 6 (8 cases)
2 * 8 = -.7
15.3
L1
1 * 7 = 6.2
1 * 5 = 4.2
3 * 3 = 2.8
2 * 4 = 1.8
3 * 9 = .7
2 * 4 = -6.3
1 * 5 = -4.8
3 * 9 = -4.2
2 * 8 = -3.0
5 *11 = -1.4
7 *13 = -1.3
-20.1
L1
3 * 3 = 1.1
1 * 7 = .9
(g) n = 7 (9 cases)
14.6
L1
3 • 4 = 4.2
2 • 9 = 4.1
3 *10 = 3.1
1 * 8 = 1.4
4 *11 = .9
2 * 5 = .7
2 * 9 = -4.4
3 * 4 = -2.6
1 * 8 = -2.6
1 * 6 = -2.5
3 *10 = -.6
-12.3
L1
2 * 5 = 1.4
(h) n = 8 (7 cases)
1 * 9 = -.8
10.5
L1
2 * 6 = 3.1
1 * 7 = 2.0
4 *12 = 1.4
2 *10 = 1.3
3 *11 = .9
3 * 5 = .8
6 *14 = .6
1 • 9 = -6.3
3 *11 = -3.8
2 *10 = -1.5
4 *12 = -1.4
3 * 5 = -.4
-10.6
L1
2 * 6 = 2.3
1 * 7 = .6

supply from nonlinear interactions and conversions, and energy lost by dissipation. During the next 3- to 4-day period of decay (stages IV and V) both the contributions of nonlinear interactions and the residue terms are negative. The period of the life cycle of waves of wavenumbers 1 and 3 respectively is about 11.5 and 10.1 days.

In view of the important role played by the nonlinear interactions in both the growing and decaying stages of the extra-long waves, the mechanism for wave interactions is analyzed. Figs. 3a and 3c show the interaction components for composite stages (I + II) and (IV + V). In these figures notation $(n_i * n_j)$ represents the interaction between waves of wavenumber n_i and wavenumber n_j. In general, contributions of wave interactions change from positive in the energy increasing stages (I + II) to negative or negligible in the energy decreasing stages (IV + V). There is no specific dominant interaction component. However, interaction components of 3*4, 2*3, 5*6, 1*2, and 4*5 are important contributions to the amplitude oscillation of waves of wavenumber 1; while interactions 1*4, 4*7, 1*2, 3*6, and 2*5 are the major contributions to the amplitude oscillation of waves of wavenumber 3.

4.2. *Synoptic-scale waves of wavenumbers 4 to 8*

Contributions to the rate of change of kinetic energy of synoptic-scale waves of wavenumbers 4 to 8 are shown in Tables 2d to 2h. Waves of wavenumber 4 are classified here as synoptic-scale waves because of their having characteristics similar to those of the synoptic-scale waves. Like the extra-long waves, the contributions of nonlinear interactions to the synoptic-scale waves are positive in energy increasing stages I and II, and negative in energy decreasing stages IV and V. Therefore, the synoptic-scale waves also become intensified by receiving energy and decayed by losing energy through nonlinear interactions among several waves. Nevertheless, the conversion term plays a more important role in the life cycle of the synoptic-scale waves than in that of the extra-long waves, since it has relatively larger magnitude and also contributes significantly in the initial energy increasing stage (stage I) of the synoptic-scale waves. The conversion term here also has a maximum value in stage III, especially for wavenumbers 6, 7 and 8. Again, the residue term is negative in all five stages and roughly cancels the contribution by the conversion term. The average period for the synoptic-scale waves is about 6 to 8 days.

Contributions of nonlinear interaction components to the amplitude oscillations of waves of wavenumbers 4 to 8 are shown in Figs. 3d to 3h. In general, interactions involving extra-long waves are important. Major interaction contributions to both the energy increasing and decreasing stages of waves of wavenumber 4 are 1*3; of wavenumber 5 are 2*3, 3*8, and 4*9; of wavenumber 6 are 1*5, 2*4, 1*7, and 3*9; of wavenumber 7 are 3*4, 2*9, 1*8, and 3*10; of wavenumber 8 are 1*9, 3*11, 2*10, and 4*12.

4.3 *Waves of wavenumber 2*

The mechanism for the life cycle of waves of wavenumber 2 is rather different from that of the other waves. Table 2b shows the contributions to the rate of change of kinetic energy of waves of wavenumber 2. It is noted that the contribution of nonlinear interactions is negative in all five stages. Examination of the detailed nonlinear interactions in Fig. 3b reveals that it is a result of a dominant negative interactions component of 1*3 in both the energy increasing and decreasing stages. Most of the secondary interaction components, however, change from positive contributions in the energy increasing stage to negative in the energy decreasing stage, e.g. interactions 3*5, 4*6, and 1*1. As a consequence, the negative value of the resultant nonlinear interactions is smaller in energy increasing than in energy decreasing stage. In addition, the nonlinear boundary term, $BL1$, also contributes positively in the energy increasing stages. Therefore, the amplitude oscillations of waves of $n = 2$ may also be attributed to the fluctuations of the nonlinear interaction contributions. The characteristics of the conversion term of $n = 2$ waves are also very different from those of the other waves. Its magnitude is large in all five stages with no peak at stage II. The anomalous behavior of $n = 2$ waves may be attributed to the effects of ocean-continent distribution in the northern hemisphere. The residue term of $n = 2$ waves is the only term which

Fig. 3. Composite contributions of nonlinear interaction components in the energy increasing (stage I + II) and decreasing (stage IV + V) stages.

Table 2. *Contributions to the rate of change of 500 mb wave kinetic energy at individual stages. Unit in* $(m/s)^2\ day^{-1}$

(a) n = 1 (7 cases)

Terms	Stages (number of days) I (2.4)	II (1.9)	III (3.0)	IV (2.3)	V (1.9)
dK/dt	5.3	8.5	−.2	−7.0	−6.0
L_1	10.5	14.7	8.6	−2.8	−1.5
$-M_1$	.0	−.3	−.3	−.8	−.2
C	.5	3.0	5.3	4.1	4.5
BVZ	.8	−1.8	−1.1	−.5	1.3
$BL1$	−2.3	−4.9	−5.0	−.7	−2.6
RES	−4.2	−2.2	−7.7	−6.3	−7.5

(b) n = 2 (7 cases)

Terms	Stages (number of days) I (1.2)	II (1.7)	III (2.8)	IV (1.2)	V (2.3)
dK/dt	3.4	4.4	.1	−6.6	−2.9
L_1	−5.9	−1.6	−1.1	−9.4	−5.6
$-M_1$	.3	−.1	−1.6	−1.1	−.1
C	12.7	17.4	15.8	16.7	15.1
BVZ	1.4	−2.4	−1.4	1.5	−.8
$BL1$	5.3	3.7	2.9	−1.1	1.7
RES	−10.4	−12.6	−14.5	−13.2	−13.2

(c) n = 3 (7 cases)

Terms	Stages (number of days) I (1.4)	II (1.9)	III (3.9)	IV (1.8)	V (1.1)
dK/dt	3.9	6.9	.3	−8.3	−5.4
L_1	10.6	13.0	3.1	−5.1	−2.0
$-M_1$	−.1	1.2	−1.0	−2.5	.1
C	.0	8.4	10.8	11.4	7.1
BVZ	−3.9	3.3	1.2	−1.8	−1.1
$BL1$	.0	−4.6	.5	3.3	−2.8
RES	−2.7	−14.4	−14.3	−13.6	−6.7

(d) n = 4 (8 cases)

Terms	Stages (number of days) I (1.5)	II (1.1)	III (2.2)	IV (2.3)	V (1.3)
dK/dt	5.1	9.2	−.4	−3.9	−5.6
L_1	6.2	6.8	.6	−6.0	−6.4
$-M_1$	.3	2.2	.6	−.1	−.2
C	5.1	7.6	6.1	7.2	2.4
BVZ	−.1	−.4	.0	−.5	1.4
$BL1$	−.8	−.4	−2.4	.0	.6
RES	−5.6	−6.6	−5.3	−4.5	−3.4

(e) n = 5 (8 cases)

Terms	Stages (number of days) I (1.6)	II (1.0)	III (1.5)	IV (1.4)	V (1.4)
$dKdt$	4.0	7.8	−.3	−5.8	−3.7
L_1	1.8	2.4	−5.8	−2.2	−6.4
$-M_1$	.0	.4	.1	−.4	−.1
C	5.0	3.1	6.1	4.5	5.3
BVZ	.8	.0	.1	−.1	.5
$BL1$	1.0	2.8	1.4	−1.5	1.4
RES	−4.6	−.9	−2.2	−6.1	−4.4

(f) n = 6 (8 cases)

Terms	Stages (number of days) I (1.2)	II (1.3)	III (1.5)	IV (1.4)	V (2.1)
dK/dt	4.9	5.7	.4	−5.3	−3.1
L_1	3.6	8.4	−2.9	−4.9	−6.4
$-M_1$	.0	.3	−.8	−.2	−.3
C	4.6	8.5	10.4	5.9	4.5
BVZ	−1.1	−3.9	1.0	−.6	.2
$BL1$	1.3	−1.5	−1.2	−1.2	1.5
RES	−3.5	−6.1	−6.1	−4.3	−2.6

(g) n = 7 (9 cases)

Terms	Stages (number of days) I (1.1)	II (1.0)	III (1.9)	IV (1.1)	V (1.2)
dK/dt	5.5	8.4	−.8	−5.3	−5.7
L_1	6.4	7.4	−2.7	−5.1	−5.4
$-M_1$	.0	−.8	−.4	−.3	−.1
C	3.5	9.6	17.1	10.4	7.7
BVZ	−1.1	−2.1	−1.7	−2.3	−2.2
$BL1$	−1.6	−1.2	.8	2.0	.9
RES	−1.7	−4.5	−13.9	−10.0	−6.6

(h) n = 8 (7 cases)

Terms	Stages (number of days) I (1.6)	II (.7)	III (1.1)	IV (1.1)	V (1.4)
dK/dt	3.0	8.7	−.4	−4.3	−4.6
L_1	2.6	8.7	−5.3	−6.1	−2.9
$-M_1$	−.1	.0	−.3	−.7	.2
C	4.8	13.3	17.3	14.0	6.1
BVZ	−.6	−1.2	1.1	.1	−.6
$BL1$	−.4	−.7	−.1	−.6	−1.1
RES	−3.3	−11.4	−13.1	−11.0	−6.3

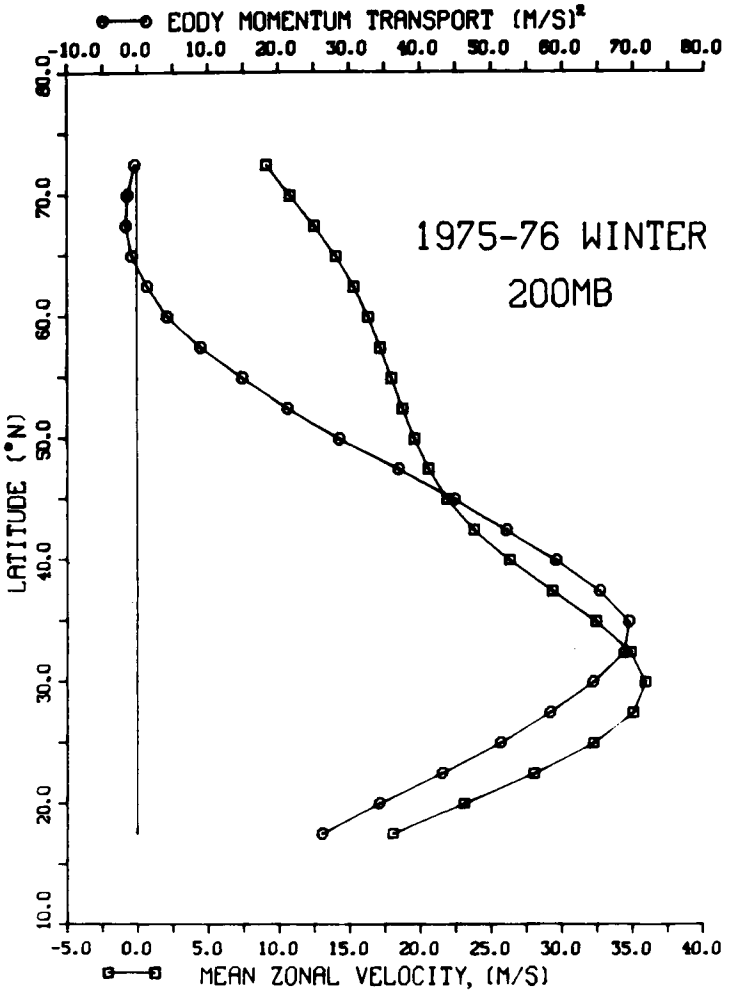

Fig. 4. Meridional distributions of average zonal wind and eddy momentum transport.

behaves similarly to that of the other waves. It is negative in all stages and also cancels most of the contribution of the conversion term.

5. Energetics of the subtropical jet stream

In this section, an analysis is made on the growth and decay of the subtropical jet stream at 200 mb. Let us examine first the meridional distributions of mean zonal wind and eddy momentum transport as shown in Fig. 4. The mean zonal wind shows a maximum value near 30°N, while the mean eddy momentum transport reaches its maximum between 32.5° and 35°N. Accordingly, we choose a latitude belt of 20°–45°N as the integration domain of the subtropical jet stream. We first compute each term in equation (1) at every 12 h of observation time, then calculate the seasonal and composite averages of each term. These seasonal averages are shown in the last column of Table 3. It is clearly seen that the subtropical jet stream is maintained by receiving kinetic energy mainly from waves ($\sum M_1 = 9.4$ m^2 s^{-2} day^{-1}) of wavenumbers 1, 5, and 6 (5.7, 1.2, and 0.9 m^2 s^{-2} day^{-1}, respectively). The maintenance of the subtropical jet stream is also contributed partly by the convergence of momentum flux ($\sum F_1 = 2.3$ m^2 s^{-2} day^{-1}). These two contributions are balanced by the energy lost through the residue term (RES $= -11.1$ m^2 s^{-2} day^{-1}). The conversion from zonal mean available

potential energy to kinetic energy is small. The contributions of the uncomputed terms $BVK(0)$ and $BWK(0)$ could be estimated from the seasonal average values of $\bar{u}$, $\bar{v}$, and $\bar{\omega}$ by Oort & Rasmusson (1971). They are both of the order of 10 $m^2 s^{-2} day^{-1}$, but opposite in sign. Therefore, on the seasonal average, the meridional convergence of zonal mean kinetic energy near the subtropical jet stream is cancelled by the vertical divergence. The other uncomputed terms were found to be small.

Table 3. *Contributions to the rate of change of kinetic energy of 200 mb zonal mean motion for individual stages and for seasonal average. Unit in* $(m/s)^2\ day^{-1}$

Terms	Stages (number of days) II (3.7)	III (4.7)	IV (2.3)	Seasonal average
dK/dt	24.8	−1.1	−30.4	1.5
$\sum_{n=1}^{20} M_1(n)$	13.9	7.7	11.4	9.4
C	.1	3.8	4.8	.9
$\sum_{n=1}^{20} F_1(n)$	18.3	4.5	−16.8	2.3
RES	−7.5	−17.1	−29.8	−11.1

The amplitude of the subtropical jet stream also oscillated with time as shown in Fig. 5. It is seen that the energy is never less than half of the peak value in the cycle. Therefore, there are no stages I and V in the life cycle of the subtropical jet oscillation. Five cases are selected for the composite averages. The results of these averages in stages II, III, and IV are also shown in Table 3. We find that the linear interaction term, $\sum M_1$, is positive in all three stages, whereas the conversion term, C, is generally small. However, the most interesting thing is that the boundary momentum flux term, $\sum F_1$, is positive in the energy increasing stage (stage II), and negative in the energy decreasing stage (stage IV). Therefore, the intensification and decay of the subtropical jet stream are respectively the effect of the convergence and divergence of eddy momentum flux. A similar phenomenon has been observed by Mintz & Kao (1952) and Lorenz (1952). The oscillation period is about 11 days. Table 4 shows the contributions of $\sum F_1$ by individual waves. It is seen that the change of $\sum F_1$ from positive in stage II to negative in stage

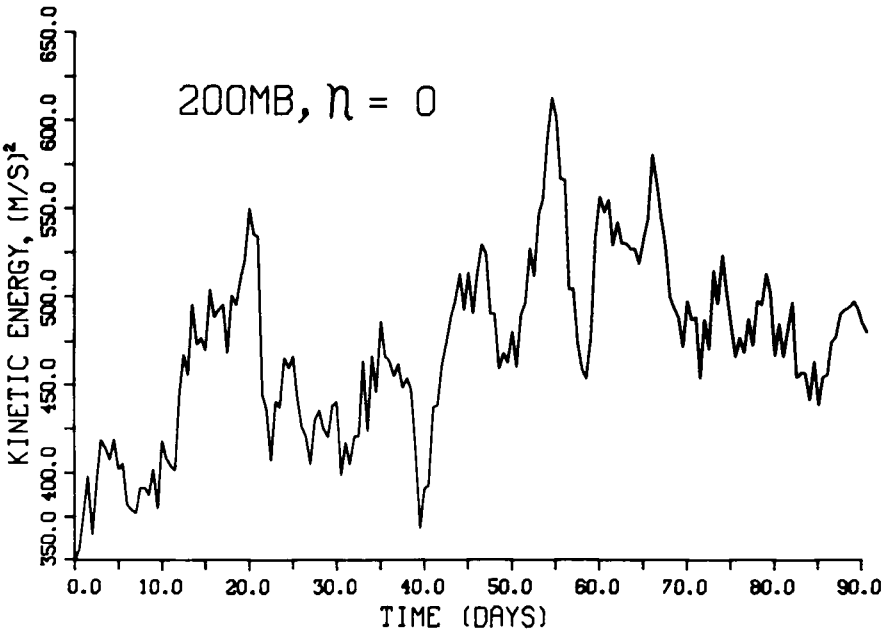

Fig. 5. Time evolutions of kinetic energies of the subtropical jet stream in the period of 1 December 1975 00Z to 29 February 1976 12Z.

Table 4. *Contributions to $F_1(n)$ from each individual wave*

Wave number	Stages (number of days) II (3.7)	III (4.7)	IV (2.3)
1	9.1	7.7	11.2
2	3.3	3.6	6.2
3	−4.8	−4.0	−19.4
4	−.8	−8.7	−7.4
5	1.9	5.8	−.3
6	4.5	−2.4	−5.2
7	.8	1.2	−3.0
8	2.0	1.7	.1

IV is mainly contributed by the synoptic-scale waves of wavenumbers 4 to 8.

6. Conclusions and discussion

An analysis of the mechanism for the wave motion in the atmosphere indicates that the energy transfers for the growth and decay of the large-scale atmospheric waves are quite different from those predicted by the linear baroclinic instability theory. In the real atmosphere, except for waves of wavenumber 2, the growth and decay of the extra-long and synoptic scale waves depend respectively on gaining and losing kinetic energy through non-linear interactions of finite amplitude waves. In the case of the synoptic scale waves, however, the baroclinic effect contributes as much as the nonlinear interactions to the initial growth of the waves. During the stage of decay, these waves reduce their amplitude by losing kinetic energy through nonlinear interactions and dissipation. An analysis of the mechanism for the growth and decay of waves of wavenumber 2 indicates that these waves always gain kinetic energy through conversion of the available potential energy, and lose energy through nonlinear interactions. This anomalous characteristic may be attributed to the effect of land-sea distribution in the northern hemisphere.

REFERENCES

Burrows, W. R. 1976. A diagnostic study of atmospheric spectral kinetic energetics. *J. Atmos. Sci. 33*, 2308–2321.

Fjørtoft, R. 1953. On the changes in the spectral distribution of kinetic energy for two-dimensional, non-divergent flow. *Tellus 5*, 225–230.

Holton, J. R. 1972. *An introduction to dynamic meteorology*. Academic Press, New York.

Kao, S.-K. 1968. Governing equations and spectra for atmospheric motion and transports in frequency wavenumber space. *J. Atmos. Sci. 25*, 32–38.

Kao, S.-K. and Lee, H.-N. 1977. The nonlinear interactions and maintenance of the large-scale moving waves in the atmosphere. *J. Atmos. Sci. 34*, 471–485.

Kao, S.-K. and Wendell, L. L. 1970. The kinetic energy of the large-scale atmospheric motion in wavenumber-frequency space: I. Northern Hemisphere. *J. Atmos. Sci. 27*, 359–375.

Lorenz, E. N. 1952. Flow of angular momentum as a predictor for the zonal westerlies. *J. Meteor. 9*, 152–157.

Lorenz, E. N. 1960. Maximum simplification of the dynamic equations. *Tellus 12*, 243–254.

Mintz, Y. and Kao, S.-K. 1952. A zonal index tendency equation and its application to forecasts of the zonal index. *J. Meteor. 9*, 87–92.

Oort, A. H., and Rasmusson, E. M. 1971. Atmospheric circulation statistics. NOAA Prof. Paper 5, U.S. Dept. of Commerce.

Saltzman, B. 1957. Equations governing the energetics of the large scales of atmospheric turbulence in the domain of wavenumber. *J. Meteor. 14*, 513–523.

Saltzman, B. 1970. Large-scale atmospheric energetics in the wavenumber domain. *Rev. Geophys. Space Phys. 8*, 289–302.

Saltzman, B. and Fleisher, A. 1960. The exchange of kinetic energy between larger scales of atmospheric motion. *Tellus 12*, 374–377.

Saltzman, B. and Fleisher, A. 1961. Further statistics on modes of release of available potential energy. *J. Geophys. Res. 66*, 2271–2273.

Steinberg, H. L., Wiin-Nielsen, A. and Yang, C.-H. 1971. On nonlinear cascades in large-scale atmospheric flow. *J. Geophys. Res. 76*, 8629–8640.

Tenenbaum, J. 1976. Spectral and spatial energetics of the GISS model atmosphere. *Mon. Wea. Rev. 104*, 15–30.

Tsay, C.-Y. and Kao, S.-K. 1973. An investigation of the spectral structure of atmospheric waves near a jet stream. *Tellus 25*, 111–131.

Tsay, C.-Y. and Kao, S.-K. 1974. An analysis of wave structure near center of maximum turbulent kinetic energy. *Tellus 26*, 299–312.

Wendell, L. L. 1969. A study of the large-scale atmospheric turbulent kinetic energy in wavenumber-frequency space. *Tellus 21*, 760–788.

Wiin-Nielsen, A. 1967. On the annual variation and spectral distribution of atmospheric energy. *Tellus 19*, 549–559.

Yang, C.-H. 1967. Nonlinear aspects of the large-scale motion in the atmosphere. Univ. Mich. Tech. Rept., 08759-1-T.

ВКЛАД ЛИНЕЙНОСТИ И НЕЛИНЕЙНОСТИ В РОСТ И ЗАТУХАНИЕ КРУПНОМАСШТАБНЫХ АТМОСФЕРНЫХ ВОЛН И СТРУЙНОГО ТЕЧЕНИЯ

Для изучения роста и затухания атмосферных волновых движений в средних широтах мы проанализировали механизм изменения кинетической энергии в пространстве волновых чисел и вычислили среднее значение каждого члена в уравнении кинетической энергии на различных стадиях жизненного цикла атмосферных волн. Найдено, что в первые два дня ультрадлинные волны с волновыми номерами 1–3 растут, получая кинетическую от других волн конечной амплитуды посредством нелинейных взаимодействий; в последующие два дня они растут как за счет того же процесса, так и за счет преобразования доступной потенциальной энергии в кинетическую. Эти волны затем поддерживают максимум энергии в течение 3–4 дней путем баланса между приходом энергии за счет указанных двух процессов и потерей энергии за счет трения. Затем вклад нелинейных взаимодействий становится отрицательным, и в следующие 3–4 дня волны затухают, теряя энергию посредством нелинейных взаимодействий и диссипации. В среднем жизненный цикл этих ультрадлинных волн составляет 10–11 дней. Аналогичные результаты были получены для волн синоптического масштаба с волновыми номерами 4–8. Они также усиливаются, получая энергию, и затухают, теряя энергию за счет нелинейных взаимодействий с другими волнами конечной амплитуды. Тем не менее преобразование доступной потенциальной энергии в кинетическую играет более важную ролъ на стадии роста для волн синоптического масштаба, чем для ультрадлинных волн. Средний жизненный цикл для волн синоптического масштаба составляет 6–8 дней. Интересно отметить, что характеристики волн с волновым номером 2 полностью отличны от характеристик других волн. На всех стадиях жизненного цикла этих волн вклад нелинейных взаимодействий отрицателен и член с преобразованием энергии всегда имеет большое положительное значение. Мы также проанализировали интенсификацию и затухание субтропического струйного течения и нашли, что они подвержены сильному воздействию конвергенции и дивергенции вихревого потока импульса. Флуктуации полного потока импульса вызываются, главным образом, волнами синоптического масштаба с волновыми номерами 4–8.